

Supplementary Materials:

Supplement 1: Properties of Fluorescent Particles

Particle name	Part number	Mean (μm)	S.D. (μm)	Filter excitation (nm)	Dichroic Mirror	Barrier Filter
Gt anti-Ms IgG (H&L)	MFP-2070-5	2.05	0.303	590-650	660	663-738
Biotin pink	TFP-5058-5	6.201	1.153	528-553	565	590-650
Biotin yellow	TFP-7052-5	7.368	0.591	490-510	515	520-550
Fluorescent Yellow	FP-3052-2	3.246	0.554	465-495	505	515-555
Fluorescent Nile Red	FP-3056	3.272	0.506	528-553	565	590-650
Fluorescent Sky blue	FP-3070-2	3.358	0.662	590-650	660	663-738

Supplement 2: Pneumatic Sample Vials

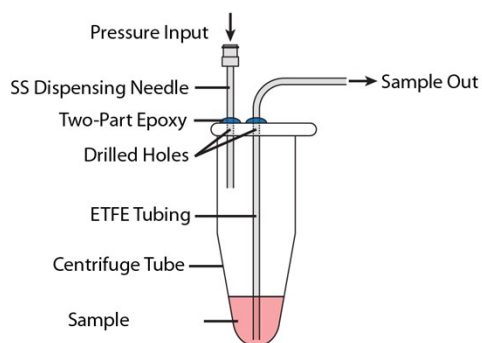


Fig. S1: Diagram of modifications to centrifuge tube for delivering sample to variable height channels. The pneumatic pressure to the pressure input is controlled to adjust the driving force and hence flow rate of the sample to the device.

Supplement 3: Image Analysis

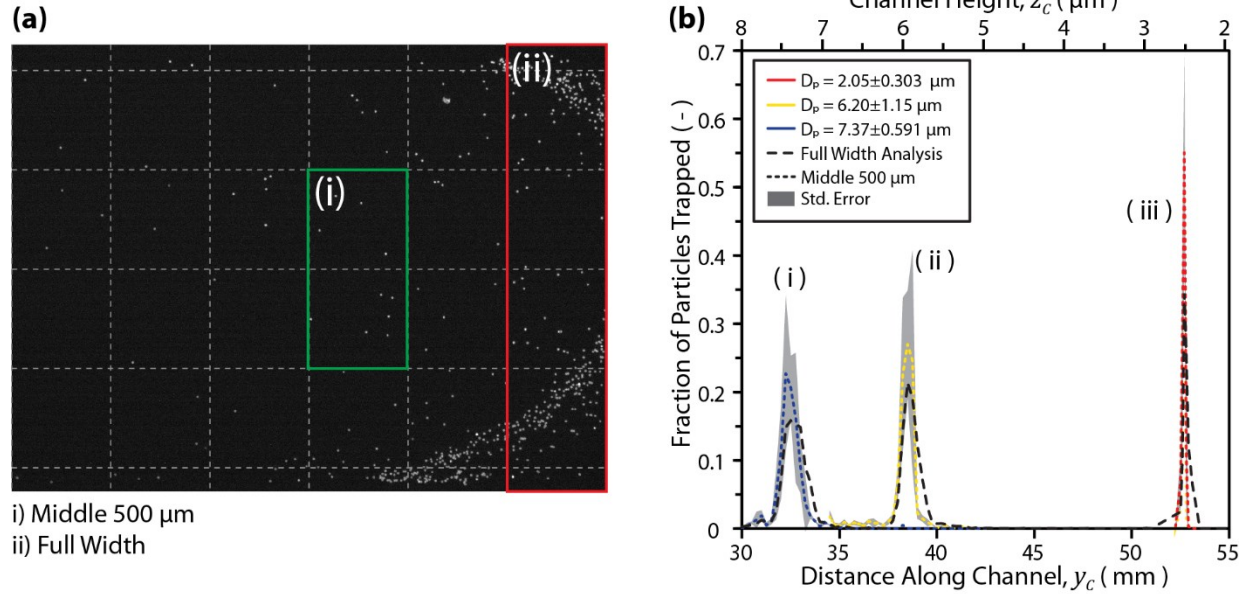


Fig. S2: Influence of image analysis on measured distribution of particles. a) Image of channel with 250 μm grid overlaid and typical areas for particle counting shown with green and red boxes. The green box encompasses the middle 500 μm of the channel and the red box the whole channel. b) The fraction of particles trapped at different positions within the channel is not significantly affected by the image analysis method, however particle counting with the full channel width shifts the measured distributions down the channels slightly due to the particles at the edge moving further down the channel for reasons discussed elsewhere.

Supplement 4: Derivation of Equations for Channel Height

a. Constant Velocity

The change in the height of the channel over time (i.e. the etch rate) can be defined as:

$$\frac{dz_c}{dt} = R$$

The speed of the wafer moving into the etchant can be expressed as a function of position (note this speed is negative with respect to the co-ordinate system chosen in Fig. 1b), with the speed being the rate of change of position over time:

$$s = \frac{dy_c}{dt} = s(y_c)$$

$$dt = \frac{-dy_c}{s(y_c)}$$

Substituting this equation into the definition of the etch rate gives an equation relating the change in the channel height to the position in the channel:

$$dz_c = \frac{-R}{s(y_c)} dy_c$$

Evaluating the indefinite integral gives the general form for the channel height for any arbitrary speed profile, $s(y_c)$:

$$z_c = -R \int \frac{dy_c}{s(y_c)}$$

This equation can be used to evaluate the etching profile for any arbitrary velocity function input. For the case where the velocity is constant for the entire wafers movement into the etchant (i.e. $s(y_c) = s$

$$z_c = -R \int \frac{dy_c}{s}$$

Evaluating the indefinite integral:

$$z_c = \frac{-R}{s} y_c + C_1$$

We define the boundary conditions for this as the channel height being zero at the final position (i.e. the wafer is not etched at any position which was not submerged in etchant solution):

$$z_c = 0 @ y_c = y_{c,f}$$

Substituting and solving yields the equation for the channel height as a function of position along the channel:

$$z_c = \frac{R}{s} (y_{c,f} - y_c)$$

Since this equation results in negative values for $y_c > y_{c,f}$ we incorporate the unit step function such

$$z_c = \frac{R}{s} (y_c - y_{c,f}) u(y_c - y_{c,f})$$

that the etch depth is always greater than or equal to zero:

Taking into account the second etch step we can add the height for a conventional etching process, Rt_{etch} globally to this:

$$z_c = \frac{R}{s} (y_c - y_{c,f}) u(y_c - y_{c,f}) + Rt_{etch}$$

b. Non-Constant Velocity

For the case of a uniformly accelerating velocity profile, i.e. $s(y_c) = ay_c + s_0$. Substitution of this velocity function into the general form, integrating with the same boundary conditions (i.e. $z_c = 0 @ y_c = y_{c,f}$), and rearranging yields:

$$z_c = -\frac{R}{a} \log\left(\frac{ay_c + s_0}{ay_{c,f} + s_0}\right)$$

Similarly for a parabolic velocity profile, i.e. $s(y_c) = ay_c^2 + by_c + s_0$, the channel height as a function of position is given by:

$$z_c = \frac{2R}{(\sqrt{4as_0 - b^2})} \left(\tan^{-1} \left(\frac{2ay_c + b}{\sqrt{4as_0 - b^2}} \right) - \tan^{-1} \left(\frac{2ay_{c,f} + b}{\sqrt{4as_0 - b^2}} \right) \right)$$

Supplement 5: Effect of Etch Parameters on Channel Profile

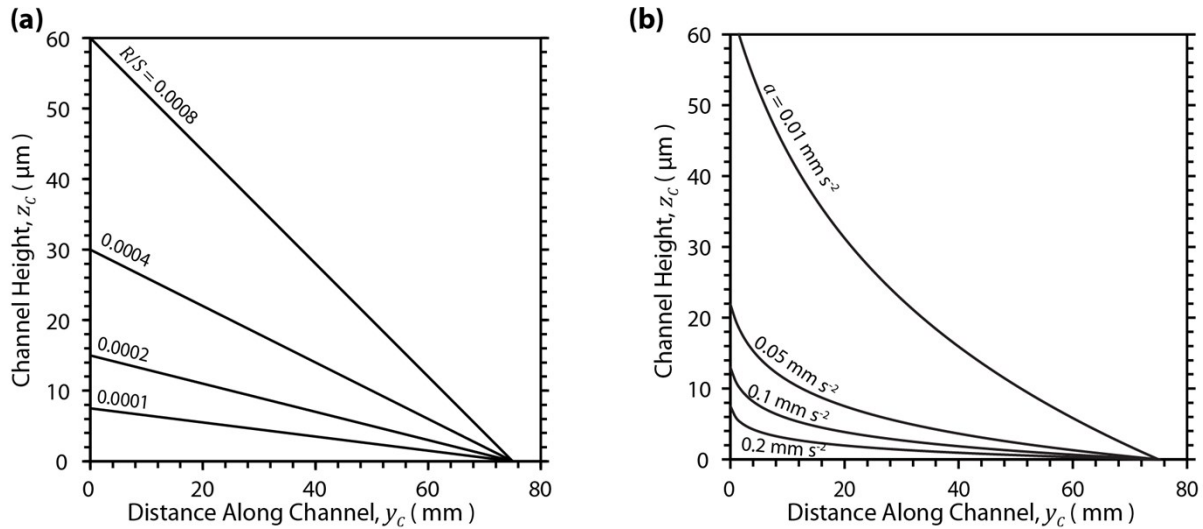


Fig. S3: Theoretical effect of fabrication parameters on the channel height. a) For wafers moving into the liquid with constant velocity, the ratio of etch rate to lowering velocity (R/S) determines the slope of the channel. Increasing R/S either by decreasing the velocity the wafer is lowered at or increasing the etch rate of the solution will result in deeper channels with higher slopes. b) Wafers which are accelerated into the etchant can obtain curved height profiles. The curvature of the height profile is dependent on the acceleration, a . As a decreases (i.e. approaches zero) the height profile tends towards the constant velocity case shown in (a).

Supplement 6: Effect of Surface Tension on Etch Profile

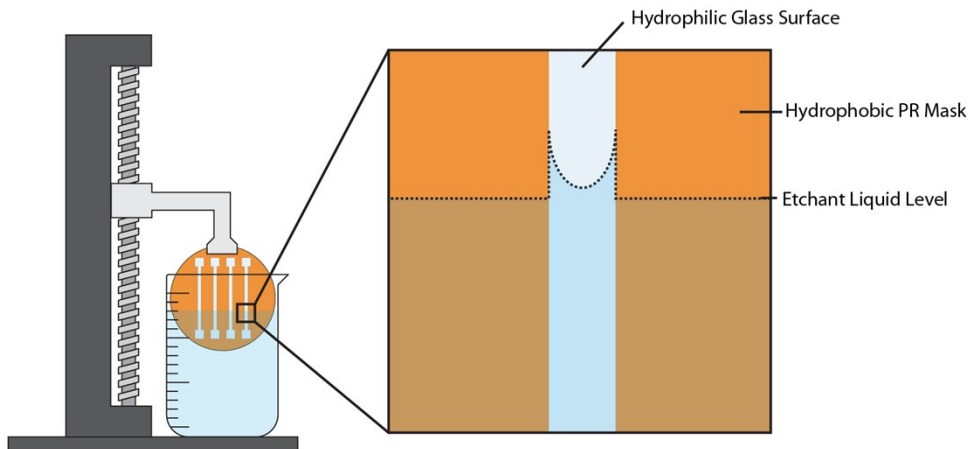


Fig. S4: Diagram highlighting the surface tension effects observed during etching. Adhesive forces between the hydrophilic glass substrate and liquid HF etchant cause the etchant to be drawn slightly upward during etching. This causes the edges of the channels to be exposed to the etchant for slightly longer, resulting in visible height variation across the width of the channel.

Supplement 7: Wafer-to-wafer Variability of Variable-height Fabrication Method

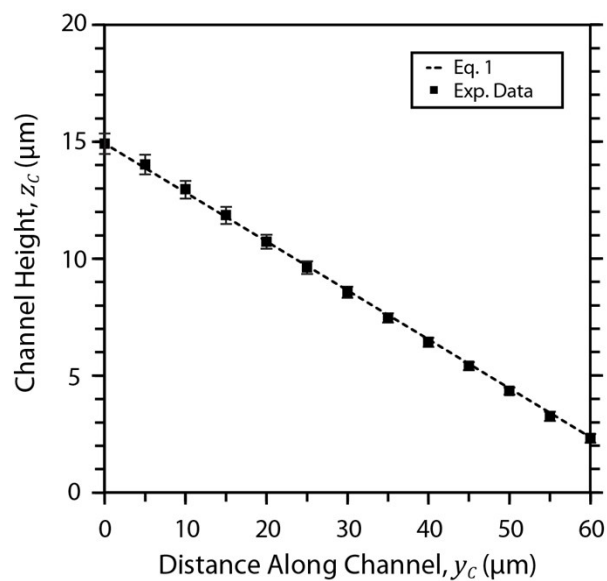


Fig. S5: Average measured height of variable height channels created with five distinct wafers using a lowering speed of ~ 1.8 mm/min into 20% w/w HF and post-etching for 2.25 min. Error bars are at the 95% confidence interval.

Supplement 8: Negative Result for Separation of Particles

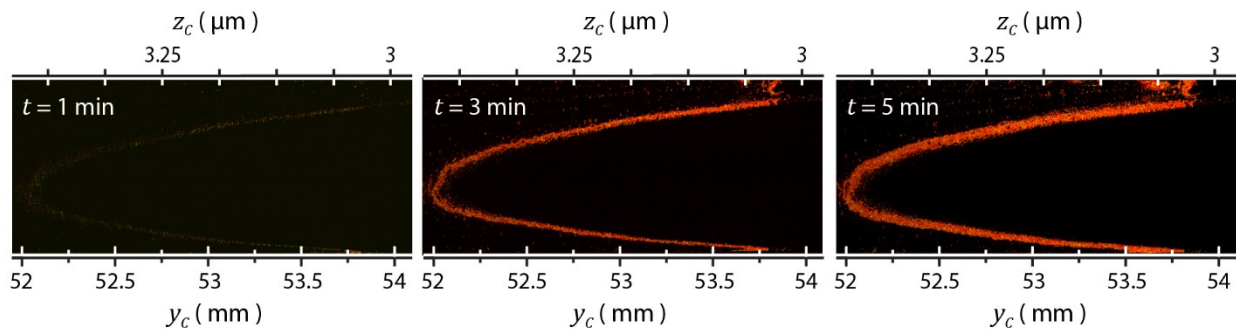


Fig. S6: Microscopic images showing the trapping of two closely-sized fluorescent particles. $3.272 \pm 0.506 \mu\text{m}$ (red) and $3.246 \pm 0.554 \mu\text{m}$ were flowed from left to right and pictures captured at 1 min, 3 min and 5 min of flow. The particles are trapped in a single band instead of two indicating the inability of this device to separate particles with these size distributions.

Supplement 9: Effect of Glutaraldehyde Treatment on RBC Size

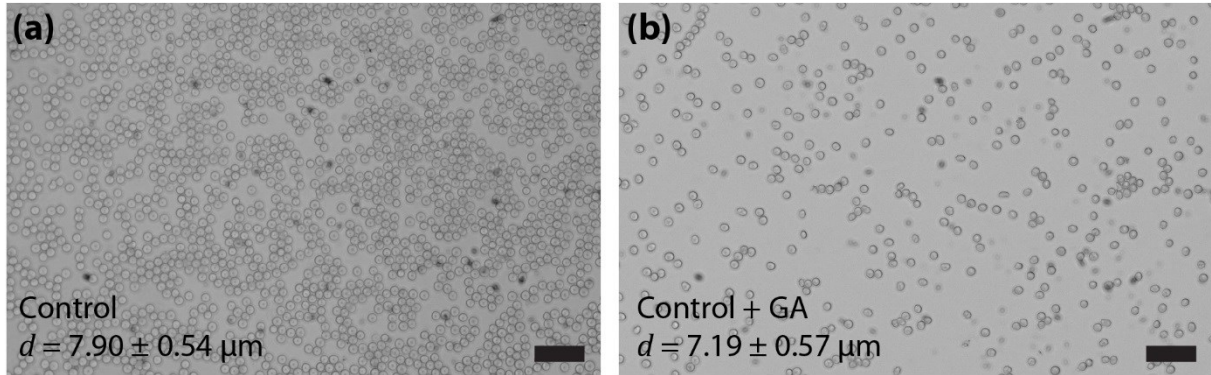


Fig. S7: Microscope images of red blood cells (a) control (b) after incubation with a glutaraldehyde solution for one hour. The diameter (d) of 60 cells was manually measured using ImageJ, and the results are presented as the average \pm the standard error. Scale bars are $50 \mu\text{m}$.

Supplement 10: Replicates of RBC Deformability Testing from Different Blood Samples

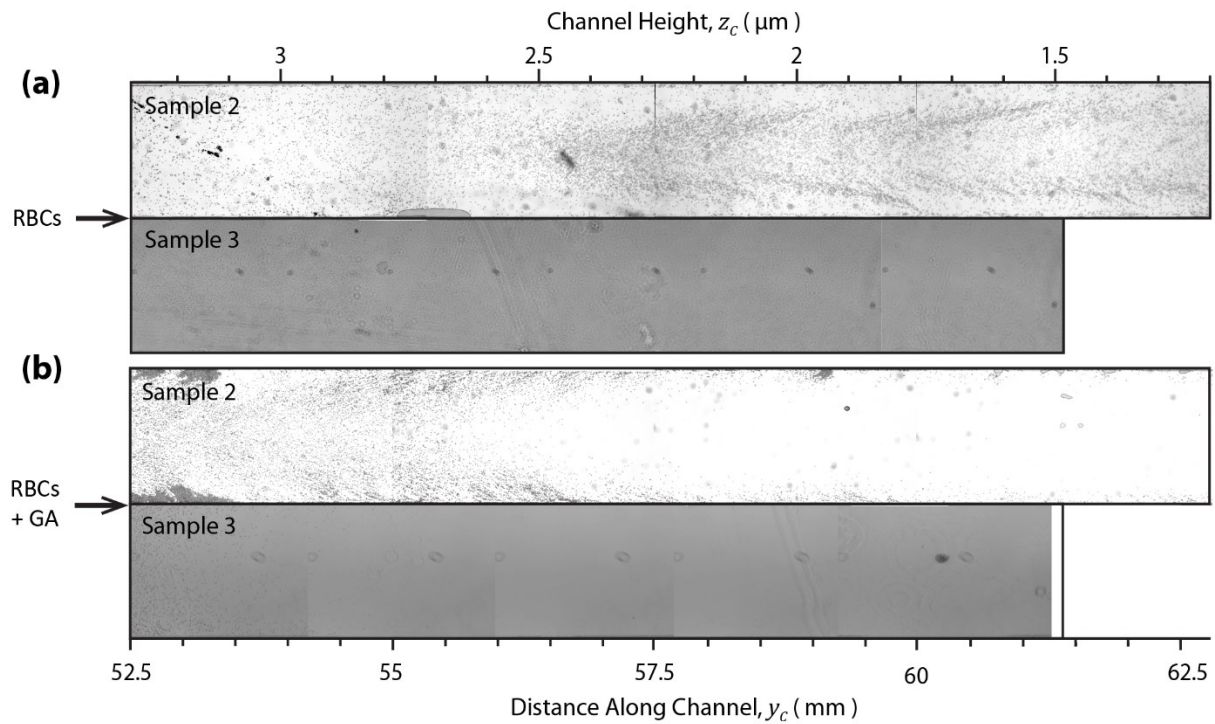


Fig. S8: Microscopic images of two additional samples showing the stopping positions of (a) healthy Red Blood Cells (RBCs) and (b) chemically modified RBCs with the addition of glutaraldehyde (GA) to decrease their deformability when flowed into two different channels at a pressure of 37.2 kPa . The healthy cells can travel through heights smaller than $1.5 \mu\text{m}$ while the cells with reduced deformability stopped at deeper channel heights.